

High-Purity Green Hydrogen Production by Bio-oil/Ethanol Mixtures Steam Reforming in Pd-Based Membrane Reactors

Sergio Iglesias-Vázquez^{a*}, José Valecillos^a, Aingeru Remiro^a, Leire Landa^a, David Alique^b, Alejandro J. Santos-Carballes^b, Raúl Sanz^c, José Antonio Calles^b, Javier Bilbao^a, Ana G. Gayubo^a

^a Univ. of the Basque Country, Dep. of Chemical Engineering, P.O. Box 644, 48080 Bilbao, Spain

^b Rey Juan Carlos University, Dep. of Chemical, Energy, and Mechanical Technology, 28933 Móstoles, Spain

^c Rey Juan Carlos University, Dep. of Chemical and Environmental Technology, 28933 Móstoles, Spain
sergio.iglesias@ehu.eus

The use of a membrane reactor (MR) for the reforming of biomass derived oxygenates is a promising approach to produce pure hydrogen from renewable sources. In this study, a Pd membrane supported on a porous stainless-steel (PSS) tube was fabricated by Electroless Pore Plating (ELP-PP) and tested in the steam reforming (SR) of bio-oil stabilized with 25 wt.% ethanol. All reaction tests were conducted in a reaction setup with two consecutive steps: (i) the thermal treatment for the vaporization of the bio-oil/ethanol mixture and the controlled deposition of pyrolytic lignin, and (ii) the SR reaction in an upwards-flow bed reactor with a Ni-based catalyst obtained upon reduction of a NiAl₂O₄ spinel. The Pd membrane was allocated in the middle of the SR reactor for its use as a MR. The reaction conditions were maintained at 580 °C with steam/carbon ratio of 2.5, space time of 0.15 h, feed pressure in the range of 1-3.3 bar, 0.1 bar in the permeate side, and time on stream of 4 h. The results reveal the enhancement of the hydrogen yield when using the MR at 3.3 bar and with the lowest gas velocity, allowing a hydrogen recovery of 57.74% with 99.8% purity. Consequently, the total hydrogen production in the MR operating at 3.3 bar and 0.6 cm s⁻¹ increased from 0.309 to 0.367 g H₂ (g C)⁻¹ if compared to the conventional reactor at 1 bar and 0.9 cm·s⁻¹.

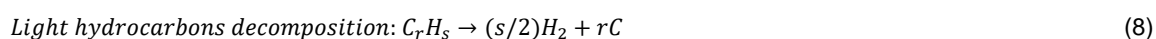
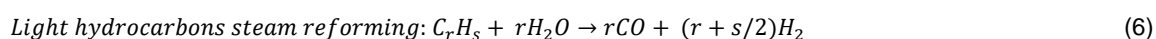
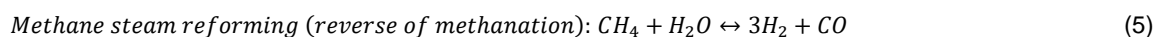
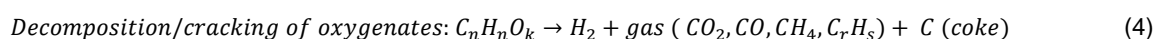
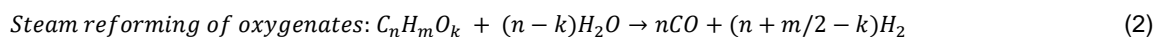
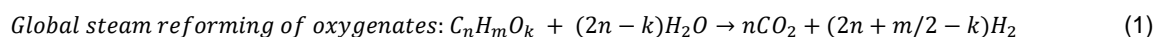
1. Introduction

Nowadays, depletion of fossil fuels, stricter environmental regulations to reduce net CO₂ emissions and a growing environmental awareness have promoted the interest on the energy production from renewable sources, with H₂ playing a crucial role in the transition from a fossil fuel based economy to a decarbonized one (Ishaq et al., 2022). In this context, the H₂ production from lignocellulosic biomass is an interesting and cleaner alternative to the main common industrial route for H₂ production based on natural gas steam reforming (NGSR), being considered as a complementary strategy to H₂O electrolysis that can improve the forestry and agricultural waste management with a neutral carbon footprint (Lepage et al., 2021). Among all different H₂ production routes from biomass, the reforming of biomass derived oxygenates is of special interest, particularly those based on bio-ethanol (Chen et al., 2023) and bio-oil (Pafili et al., 2021). Bio-ethanol is non-toxic and easy to store and handle, has a high H₂ content, high reactivity even at low temperature, and there are encouraging prospects for its large-scale production from lignocellulosic biomass (Lamichhane et al., 2021). Likewise, bio-oil can be produced with low operating costs and relatively simple equipment in a delocalized way, i.e. through well-developed fast pyrolysis technologies (Baloch et al., 2018). As both oxygenated feeds are more energy dense and easier to transport than biomass, their reforming could be centralized in a bio-refinery with units designed *ad-hoc* for the selective H₂-production. The SR of a mixed bio-oil/bio-ethanol feed is an interesting strategy due to the following reasons: (i) ethanol can help to stabilize the bio-oil during its storage instead of the more common methanol (Yi et al., 2021); (ii) ethanol co-feeding has a favourable effect on the SR of raw bio-oil, mitigating the problems caused by pyrolytic lignin deposition and coke deactivation (Remiro et al., 2014); and (iii) the operating conditions to maximize H₂ yield with both oxygenated feeds are similar (Montero et al., 2015).

Paper Received: 7 February 2023; Revised: 27 April 2023; Accepted: 27 May 2023

Please cite this article as: Iglesias-Vazquez S., Valecillos J., Remiro A., Landa L., Alique D., Santos-Carballes A.J., Sanz R., Calles J.A., Bilbao J., Gayubo A.G., 2023, High-purity Green Hydrogen Production by Bio-oil/ethanol Mixtures Steam Reforming in Pd-based Membrane Reactors, Chemical Engineering Transactions, 100, 259-264 DOI:10.3303/CET23100044

The overall stoichiometry of SR of oxygenates in bio-oil (Eq. (1)), which also applies to ethanol ($n = 2$, $m = 6$ and $k = 1$), is a combination of the stoichiometry for partial SR (Eq. (2)) and water gas shift (WGS) (Eq. (3)) reactions, with other reactions taking place in parallel (Eqs. (4)-(10)).



Ni-based catalysts, especially those derived from $NiAl_2O_4$ spinel, have a high activity for bio-oil reforming and possibility to be completely regenerated (Landa et al., 2023). However, the challenge of maximizing the H_2 formation not only requires the use of highly active and selective catalysts that avoid undesired secondary reactions (Eqs. (4), (7), (8) and (9)) responsible of the catalyst deactivation, but also depends on the thermodynamic equilibria of methane SR (SRM) and WGS reactions, which can be promoted using selective membranes. The use of a membrane reactor (MR) permeable to H_2 enables its continuous extraction from the reaction medium, producing a pure hydrogen stream on the permeate side. This fact shifts the thermodynamic equilibrium of SRM and WGS towards products, thus increasing the feed conversion and H_2 yield compared to a conventional reactor. The benefits of using a MR has been extensively reported with methane (Nalbant Atak et al., 2021), biogas (Iulianelli et al., 2021) or ethanol (Taghizadeh and Aghili, 2019) feeds, but there are no previous references concerning the use of MR for bio-oil SR.

The membranes based on Pd or Pd-based alloys are especially attractive due to their theoretical complete H_2 selectivity, high permeability and reasonable mechanical stability (Habib et al., 2021). A low Pd-thickness is of key importance for reducing its production cost while improving the H_2 flux through the membrane. Thin Pd membranes can be prepared by supporting the thin Pd-film onto porous stainless steel (PSS) to provide enough mechanical resistance and thermal stability (Kiadehi and Taghizadeh, 2019). Due to the original roughness and wide pore size distribution of these supports, the incorporation of ceramic particles as intermediate layer between both PSS support and Pd layer favours the generation of a smoother surface with smaller pores, thus reducing the required amount of Pd for a fully dense layer. In addition, this strategy also prevents any intermetallic diffusion from steel to Pd during the membrane operation at high temperatures (Martinez-Diaz et al., 2022).

Under this perspective, the objective of the current research is to evaluate the SR of a bio-oil/ethanol mixture in a MR equipped with a composite Pd/PSS membrane containing a CeO_2 intermediate layer between both PSS support and Pd-film, and its comparison with the results obtained in a conventional reactor.

2. Materials and methods

2.1 Catalyst synthesis

The $NiAl_2O_4$ spinel precursor was synthesized by the co-precipitation of nickel nitrate with aluminum nitrate and NH_4OH as the precipitating agent, as detailed elsewhere (Landa et al., 2023). The precursor was reduced at $850\text{ }^\circ\text{C}$ for 4 h under H_2 - N_2 flow (10 % vol. H_2) to obtain the active Ni^0 particles dispersed on the Al_2O_3 support.

2.2 Membrane synthesis

A commercial finger-like PSS tube (AmesPore, OD = 3/8", length = 73 mm, total porosity = 21%, average pore size = 1 μm) was used for the membrane fabrication. The raw support was first cleaned by three consecutive

immersions in solutions of sodium hydroxide, hydrochloric acid, and ethanol under ultrasonic stirring with intermediate rinsing in distilled water and final drying overnight at 110 °C. The clean support was calcined at 600 °C for 12 h and its surface was modified by the incorporation of a CeO₂-based layer via dip-coating from a suspension containing 10 wt.% of ceramic particles and 2 wt.% of poly(vinyl alcohol) (PVA). The modified support was calcined again (450 °C for 10 h) to ensure its stability and then the top H₂-selective film was incorporated by palladium Electroless Pore-Plating (ELP- PP) following a previously optimized procedure (Martinez-Diaz et al., 2021). Basically, the solution containing the metal source was placed around the external surface of the porous support, while a N₂H₄ solution was introduced in the lumen of the tube as reducing agent forcing the reaction to take place just inside the pores or their neighborhoods. The plating step was repeated several times until ensuring complete N₂ tightness. At these conditions, the Pd-thickness estimated by gravimetric analysis was 13.8 μm (considering the formation of a homogeneous top film).

2.3 Bio-oil

The raw bio-oil was supplied by BTG Bioliquids BV (The Netherlands) and synthesized from fast pyrolysis of pine sawdust in a conical rotatory reactor. Its main physical-chemical properties can be summarized as follows: water content, determined by using Karl-Fischer titration (KF-Titrino Plus 870), 19.82 wt%; density, 1.2 g ml⁻¹; pH, 2.42; and empirical formula C_{4.8}H_{5.7}O_{2.3} (water-free basis). The detailed raw bio-oil composition was determined with a Shimadzu QP2010S gas chromatography/mass spectrometer (GC/MS) provided with a BPX-5 column (50 m × 0.22 mm × 0.25 μm) and mass selective detector, obtaining the presence of ketones, acids, phenols, esters, saccharides, aldehydes, furans/furanones, alcohols and ethers.

2.4 Reaction equipment and operating conditions

The reaction tests were carried out in automated reaction equipment (PID Eng & Tech) provided with two units in series: the first one (downflow tube) is used for the vaporization of the oxygenated feed and the removal of the pyrolytic lignin from the bio-oil, while the second one (catalytic upflow reactor with an internal diameter of 32 mm, a total length of 305 mm and an effective reaction length of 8 mm) is dedicated for the steam reforming of the volatilized oxygenates. The reaction equipment is connected on-line to a micro gas chromatograph (MicroGC, Agilent CP 490) with three modules for the detection and quantification of products. A small fraction of the reactor outlet stream is sent to the MicroGC by means of a carrier gas (He, 30 mL min⁻¹) through a thermostated line (130 °C) to avoid condensation of products. For the MR tests, the Pd-membrane was inserted in the middle of the catalytic reactor with its open side connected to a vacuumed system (permeate). In this case, a small fraction of the outlet stream from the permeate side was also sent to the MicroGC by means of a line of carrier gas, and both streams (retentate and permeate) were periodically analyzed in the MicroGC. The mass balance was closed in all tests above 90 %.

The permeation tests of the Pd-membrane were done in the same equipment at 400 °C feeding pure H₂ and varying the pressure by means of a restricting valve.

For the reaction tests, the catalytic bed consisted of a mixture of catalyst (0.45 g) and inert solid (100 g) (carborundum), maintaining a bed height/diameter relationship of around 2. All the tests were carried out at 580 °C by feeding a mixture of bio-oil/ethanol (75/25 % w/w) with inlet flowrate of 1.77 g·h⁻¹, space time of 0.15 h, S/C molar ratio of 2.5, and oxygenates concentration of 5 % v/v (using a N₂ stream as an inert to dilute the gases) and a total reaction time of 4 h. The pressure was set in the 1.1-3.3 bar range and, when using the membrane tube, the permeate side was maintained at 0.1 bar to provide enough pressure driving force for the permeation. The upwards gas linear velocity through the reactor was varied depending on total pressure from 0.60 cm·s⁻¹, to 2.70 cm·s⁻¹, being 1.40 cm·s⁻¹ the minimum fluidization velocity.

The kinetic behavior was quantified with the molar fraction of the gaseous products, the carbon conversion (X , Eq. (11)) and H₂ yield (Y_{H_2} , Eq. (12)). In these equations, F_G is the molar flowrate of C containing gaseous products (CO₂, CO, CH₄ and light hydrocarbons, in C equivalent units), F_{Feed} is the flowrate of carbon in the feed, F_{H_2} is the H₂ molar flow rate in the product stream and $F_{H_2}^o$ is the stoichiometric H₂ molar flow rate, calculated as $(2n + m/2 - k)/n F_{Feed}$, according to the global stoichiometry for steam reforming (Eq. (1)).

$$X = \frac{F_G}{F_{Feed}} \quad (11)$$

$$Y_{H_2} = \frac{F_{H_2}}{F_{H_2}^o} \quad (12)$$

3. Results

3.1. Membrane behavior

Figure 1 collects the permeate flux reached at different transmembrane pressures, showing a good fitting to the Sieverts' law. At these conditions, a permeance value of $1.23 \cdot 10^{-4} \text{ mol} \cdot \text{s}^{-1} \cdot \text{m}^{-2} \cdot \text{Pa}^{-0.5}$ can be calculated, which is an intermediate value between those reported by Calles et al. (2018) for Pd membranes prepared by a similar procedure. This result is coherent with the intermediate value of the thickness for the Pd-film reached in this work compared to those prepared in the above-mentioned previous work. Moreover, the perm-selectivity of the membrane was tested feeding mixtures of N_2/H_2 (H_2 composition from 10 % to 90 %) at different pressures, reaching an average H_2 purity of 99.08 %, increasing up to 99.9 % at higher transmembrane pressures, with a H_2/N_2 perm-selectivity in the range 107-999.

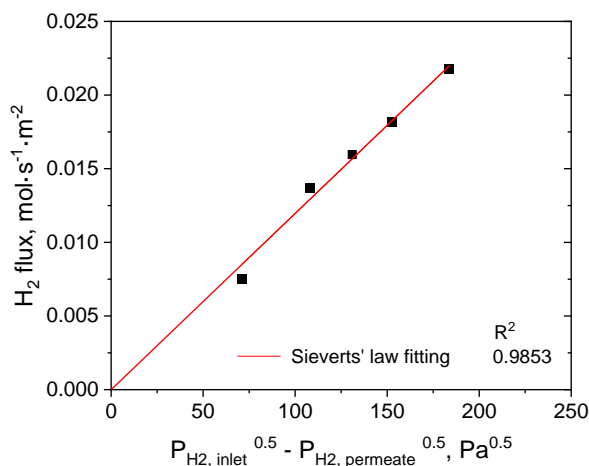


Figure 1: Permeability of the tested membrane at 400 °C.

3.2 Reaction tests

The use of a membrane reformer reactor brings up the challenge of operating at high pressures to favor the H_2 separation, as shown in Figure 1, despite its well-known negative effect on the thermodynamic of SR reactions. To prove the advantages of using a membrane reformer reactor, the reaction performance at different pressures and linear velocities (affected by the pressure) was compared with or without the use of a H_2 -selective membrane in the reaction system. Figure 2 shows the evolution with time on stream of the conversion (graph a) and H_2 yield (graph b), in the reactions carried out in conventional or membrane reactors (sum of the H_2 yield in the retentate and permeate sides).

The continuous lines in Figures 2a and 2b show the conversion and H_2 yield, respectively, for the conventional SR reactor (without membrane) operated as a fluidized bed (linear velocity of $2.70 \text{ cm} \cdot \text{s}^{-1}$, almost twice the minimum fluidization velocity of the bed, $1.40 \text{ cm} \cdot \text{s}^{-1}$) at 1.1 bar and as packed bed (linear velocity of $0.90 \text{ cm} \cdot \text{s}^{-1}$) at 1.1 and 3.3 bar. At initial time on stream, both reaction tests at 1.1 bar have complete conversion and high H_2 yield (around 85 %). However, the catalyst activity in the fluidized bed reactor decreases over time, whereas the deactivation is slower for the packed bed reactor. This behavior can be explained because of a less efficient contact between the gas fluid and catalyst particles in fluidized bed conditions, which decreases the oxygenates conversion (Landa et al., 2023). However, when operating at 3.3 bar, the reaction gains in stability at expense of a decrease in conversion and H_2 yield because the pressure worsen the SR reactions and favors methanation, according to the Le Châtelier's principle (Kızılpelit et al., 2022). Accordingly, H_2 and CO molar fractions decrease whereas those of CH_4 and CO_2 increase with pressure (as shown by the black and blue full bars of Figure 3a). In case of working with MR configuration (discontinuous lines with empty markers in Figure 2), both conversion and H_2 yield increase with pressure, obtaining complete conversion and around 90 % H_2 yield at 3.3 bar. Furthermore, the reaction carried out at a linear velocity of $0.60 \text{ cm} \cdot \text{s}^{-1}$ has also complete conversion but higher H_2 yield than the one obtained at $0.90 \text{ cm} \cdot \text{s}^{-1}$ at 3.3 bar. This result can be explained because a lower linear velocity inside the reactor allows a higher H_2 recovery, avoiding that a high bulk of H_2 bypasses the membrane (Nakajima et al., 2015).

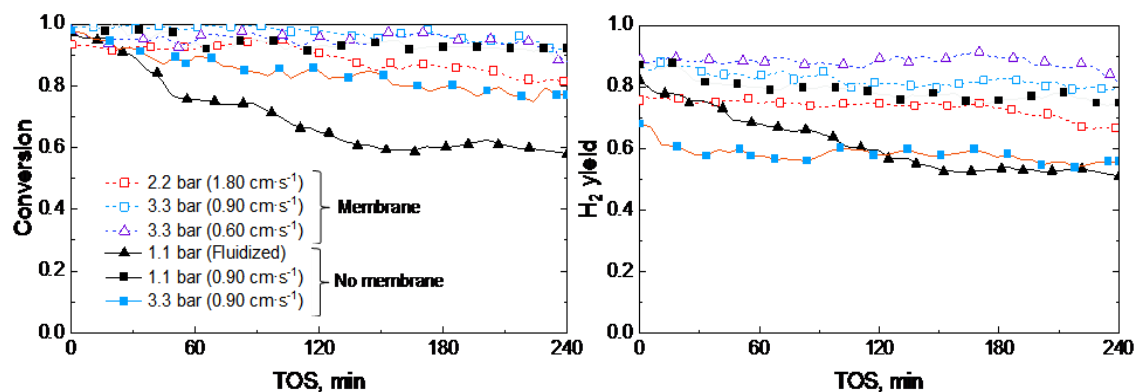


Figure 2: (a) Conversion and (b) H₂ yield of the reactions with and without membrane.

The molar fractions of the gaseous products obtained at zero time on stream without membrane and in the retentate side when using the membrane are depicted in Figure 3a, whereas Figure 3b shows the H₂ production along the reaction referred to the mass of carbon fed into the system. The molar fractions of CO₂ in the MR (Figure 3a) are higher than operating without a H₂-selective membrane and increase with pressure, whereas those of CO and CH₄ remains almost constant or decrease. These results evidence that the in-situ removal of a H₂ from the reaction medium shifts the thermodynamic equilibrium of both SRM and WGS reactions, which results in higher H₂ production (Figure 3b). Without membrane, the highest H₂ production is achieved operating the reactor as a packed bed at 1.1 bar, whereas fluidization conditions and pressure increase worsen H₂ production. On the other hand, the use of a Pd-membrane improves H₂ production compared to the reaction tests in a conventional reaction system at the same pressure (3.3 bar) and even at 1.1 bar. The pressure increase, which promotes the transmembrane pressure as main driving force for the H₂ separation, notoriously improves the H₂ recovery (more H₂ permeated). Likewise, reducing the feed flow rate to meet a linear velocity of 0.60 cm·s⁻¹ at 3.3 bar enhances the H₂ permeation and the overall H₂ production.

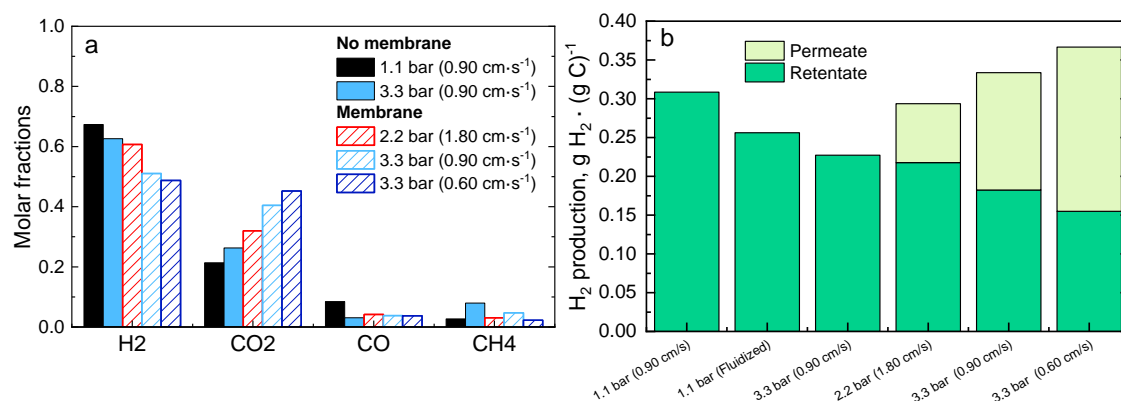


Figure 3: (a) Molar fractions of the gaseous products in the retentate stream and (b) H₂ production per mass of carbon fed into the system.

4. Conclusions

This study proves, for the first time, the benefits of using a MR equipped with a Pd-membrane for the SR of mixture containing bio-oil and ethanol. The results evidence the relevant role that pressure and gas velocity play in the MR performance. At high enough pressure, the H₂ permeate flux shifts the equilibrium of both SRM and WGS reactions, thus increasing H₂ yield. The linear velocity of the gases inside the reactor is an important factor, because its decrease minimizes the bypass of the membrane, thus enhancing the recovery of H₂ with high purity. As a result, a membrane reactor operating at 580 °C, 3.3 bar and low flowrate (0.60 cm s⁻¹) contributed to increase the H₂ production from 0.309 to 0.367 g_{H₂} (g_C)⁻¹ when compared to a conventional system working with 0.90 cm s⁻¹ at 1.1 bar. The improvement in the preparation of the Pd-membrane, by lowering its thickness and thus improving the H₂ permeation, will lead to a higher increase in the H₂ production together with the reduction of the production cost of the membrane, which is a key factor for making more attractive the process for its future scale-up.

Acknowledgments

This work was financially supported by MCIN/AEI/10.13039/501100011033 and “ERDF A way of making Europe” (grants RTI2018-100771-B-I0, PID2020-117273RB-I00, PID2021-127005OB-I00, and PhD grant BES-2019-090943), the European Union Commission (HORIZON H2020-MSCA RISE 2018, contract 823745) and the Basque Government (project IT1645-22).

References

- Baloch H.A., Nizamuddin S., Siddiqui M.T.H., Riaz S., Jatoi A.S., Dumbre D.K., Mubarak N.M., Srinivasan M.P., Griffin G.J., 2018, Recent advances in production and upgrading of bio-oil from biomass: A critical overview. *Journal of Environmental Chemical Engineering*, 6, 5101–5118.
- Calles J.A., Sanz R., Alique D., Furones L., Marín P., Ordoñez S., 2018, Influence of the selective layer morphology on the permeation properties for Pd-PSS composite membranes prepared by electroless pore-plating: Experimental and modeling study. *Separation and Purification Technology*, 194, 10–18.
- Chen W.-H., Biswas P.P., Ong H.C., Hoang A.T., Nguyen T.-B., Dong C.-D., 2023, A critical and systematic review of sustainable hydrogen production from ethanol/bioethanol: Steam reforming, partial oxidation, and autothermal reforming. *Fuel*, 333, 126526.
- Habib M.A., Harale A., Paglieri S., Alrashed F.S., Al-Sayoud A., Rao M.V., Nemitallah M.A., Hossain S., Hussien M., Ali A., Haque M.A., Abuelyamen A., Shakeel M.R., Mokheimer E.M.A., Ben-Mansour R., 2021, Palladium-Alloy Membrane Reactors for Fuel Reforming and Hydrogen Production: A Review. *Energy and Fuels*, 35, 5558–5593.
- Iulianelli, A., Manisco M., Bion N., Le Valant A., Epron F., Colpan C.O., Esposito E., Jansen J.C., Gensini M., Caravella A., 2021, Sustainable H₂ generation via steam reforming of biogas in membrane reactors: H₂S effects on membrane performance and catalytic activity. *International Journal of Hydrogen Energy*, 46, 29183–29197.
- Kiadehi A. D., Taghizadeh M., 2019, Fabrication, characterization, and application of palladium composite membrane on porous stainless steel substrate with NaY zeolite as an intermediate layer for hydrogen purification. *International Journal of Hydrogen Energy*, 44, 2889–2904.
- Kızılpelit B.G., Karaosmanoğlu F., Özkara-Aydinoğlu Ş., 2022, A thermodynamic equilibrium analysis of hydrogen and synthesis gas production from steam reforming of acetic acid and acetone blends as bio-oil model compounds. *International Journal of Hydrogen Energy*, 47, 39758–39770.
- Landa L., Remiro A., Valle B., Bilbao J., Gayubo A.G., 2023, Comparison of the NiAl₂O₄ derived catalyst deactivation in the steam reforming and sorption enhanced steam reforming of raw bio-oil in packed and fluidized-bed reactors. *Chemical Engineering Journal*, 458, 141494.
- Lepage T., Kammoun M., Schmetz Q., Richel A., 2021, Biomass-to-hydrogen: A review of main routes production, processes evaluation and techno-economical assessment. *Biomass and Bioenergy*, 144, 105920.
- Lamichane G., Acharya A., Poudel D.K., Aryal B., Gyawali N., Niraula P., Phuyal S.R., Budhathoki O., Bk G., Parajuli N., 2021, Recent advances in bioethanol production from lignocellulosic biomass. *International Journal of Green Energy*, 18, 731–44.
- Martinez-Diaz D., Leo P., Sanz R., Carrero A., Calles J.A., Alique D., 2021, Life cycle assessment of H₂-selective Pd membranes fabricated by electroless pore-plating. *Journal of Cleaner Production*, 316, 128229.
- Martinez-Diaz D., Michienzi V., Calles J.A., Sanz R., Caravella A., Alique D., 2022, Versatile and Resistant Electroless Pore-Plated Pd-Membranes for H₂-Separation: Morphology and Performance of Internal Layers in PSS Tubes. *Membranes*, 12, 530.
- Montero C., Oar-Arteta L., Remiro A., Arandía A., Bilbao J., Gayubo, A.G., 2015, Thermodynamic comparison between bio-oil and ethanol steam reforming. *International Journal of Hydrogen Energy*, 40(46), 15963–15971.
- Nakajima T., Kume T., Ikeda Y., Shiraki M., Kurokawa H., Iseki T., Kajitani M., Tanaka H., Hikosaka H., Takagi Y., Ito M., 2015, Effect of concentration polarization on hydrogen production performance of ceramic-supported Pd membrane module. *International Journal of Hydrogen Energy*, 40, 11451–11456.
- Nalbant Atak Y., Colpan C.O., Iulianelli A., 2021, A review on mathematical modeling of packed bed membrane reactors for hydrogen production from methane. *International Journal of Energy Research*, 45, 20601–20633.
- Pafili A., Charisiou N.D., Douvartzides S.L., Siakavelas G.I., Wang W., Liu G., Papadakis V.G., Goula M.A., 2021, Recent progress in the steam reforming of bio-oil for hydrogen production: A review of operating parameters, catalytic systems and technological innovations. *Catalysts*, 11, 1526.
- Remiro A., Valle B., Oar-Arteta L., Aguayo A.T., Bilbao J., Gayubo A.G., 2014, Hydrogen production by steam reforming of bio-oil/bio-ethanol mixtures in a continuous thermal-catalytic process. *International Journal of Hydrogen Energy*, 39, 6889–6898.
- Taghizadeh M., Aghili F., 2018, Recent advances in membrane reactors for hydrogen production by steam reforming of ethanol as a renewable resource. *Reviews in Chemical Engineering*, 35, 377–392.